

## High-resolution study of the Gamow-Teller strength distribution in $^{51}\text{Ti}$ measured through $^{51}\text{V}(d, ^2\text{He})^{51}\text{Ti}$

C. Bäumer,<sup>1</sup> A. M. van den Berg,<sup>2</sup> B. Davids,<sup>2</sup> D. Frekers,<sup>1</sup> D. De Frenne,<sup>3</sup> E.-W. Grewe,<sup>1</sup> P. Haefner,<sup>1</sup> M. N. Harakeh,<sup>2</sup> F. Hofmann,<sup>4</sup> M. Hunyadi,<sup>2</sup> E. Jacobs,<sup>3</sup> B. C. Junk,<sup>1</sup> A. Korff,<sup>1</sup> K. Langanke,<sup>5</sup> G. Martínez-Pinedo,<sup>6,7</sup> A. Negret,<sup>3</sup> P. von Neumann-Cosel,<sup>4</sup> L. Popescu,<sup>3</sup> S. Rakers,<sup>1</sup> A. Richter,<sup>4</sup> and H. J. Wörtche<sup>2</sup>

<sup>1</sup>*Institut für Kernphysik, Westfälische Wilhelms-Universität Münster, D-48149 Münster, Germany*

<sup>2</sup>*Kernfysisch Versneller Instituut, Rijksuniversiteit Groningen, NL-9747 AA Groningen, The Netherlands*

<sup>3</sup>*Vakgroep Subatomaire en Stralingsfysica, Universiteit Gent, B-9000 Gent, Belgium*

<sup>4</sup>*Institut für Kernphysik, Technische Universität Darmstadt, D-64289 Darmstadt, Germany*

<sup>5</sup>*Institut for Fysik og Astronomie, Århus Universitet, DK-8000 Århus, Denmark*

<sup>6</sup>*Institut d'Estudis Espacials de Catalunya, E-08034 Barcelona, Spain*

<sup>7</sup>*Institució Catalana de Recerca i Estudis Avançats, E-08010 Barcelona, Spain*

(Received 5 March 2003; published 22 September 2003)

The  $^{51}\text{V}(d, ^2\text{He})^{51}\text{Ti}$  charge-exchange reaction has been investigated at an incident energy of 171 MeV and scattering angles near  $0^\circ$ . The two protons in the  $^1S_0(pp)$  state (denoted as  $^2\text{He}$ ) were both momentum analyzed and detected by the same spectrometer and detector. Spectra with a resolution of about 125 keV (full width at half maximum) have been obtained allowing identification of many levels in  $^{51}\text{Ti}$  with high precision. The  $\text{GT}^+$  strength distribution for transitions to levels up to about 6 MeV of excitation energy has been extracted. The results are compared with a large-scale shell-model calculation in the full  $pf$  shell.

DOI: 10.1103/PhysRevC.68.031303

PACS number(s): 25.45.Kk, 21.10.Pc, 21.60.Cs, 21.60.Ka

Charge-exchange reactions using  $(p, n)$ - and  $(n, p)$ -type probes at intermediate energies ( $E/A > 100$  MeV/u) have widely been used to study spin-isospin-flip excitations in nuclei (Ref. [1] and references therein). In the limit of vanishing momentum transfer ( $\Delta L = 0, q = 0$ ) these transitions are referred to as of Gamow-Teller (GT) type. They are directly connected to the weak nuclear transitions with the additional advantage that they can probe excitation energies, which are inaccessible to the ordinary weak beta decay.

Transitions in the  $\beta^+$  direction ( $\text{GT}^+$ ) from  $pf$ -shell nuclei are of astrophysical interest as they provide important input to the modeling of the explosion dynamics of a massive star. The electron capture (EC) process, which predominantly populates  $\text{GT}^+$  states in the daughter nucleus, determines the rate of deleptonization and, ultimately, the explosive power of a supernova. The importance of the  $\text{GT}^+$  strength distribution for stellar EC was first recognized by Bethe *et al.* [2]. Later, in the parametrization of Fuller, Fowler, and Newman (FFN) [3] the EC rates for nuclei in the mass range  $A = 45$ – $60$  were systematically estimated. These tabulations are now being replaced by the results of modern large-scale shell-model calculations [4,5] and a detailed confrontation with the experimental results is of considerable importance for the supernova physics. A review of the field of nuclear weak-interaction processes in stellar evolution is given in Ref. [6].

GT transitions in the  $\beta^-$  direction ( $\text{GT}^-$ ) have extensively been studied by means of  $(p, n)$  and  $(^3\text{He}, t)$  charge-exchange reactions [7–9]. These experiments generally yielded spectra with good resolution, making the extraction of  $B(\text{GT}^-)$  relatively straightforward. On the other hand, high-resolution studies of  $\text{GT}^+$  transitions are significantly more difficult. Typical resolutions of the pioneering  $(n, p)$  experiments at TRIUMF were of the order of 1 MeV [10,11].

At some of the new radioactive ion beam facilities, triton beams at sufficiently high energies have become available, and the  $(n, p)$ -type charge-exchange  $(t, ^3\text{He})$  reaction with improved resolution appears to be a competitive tool [12,13].

The present experiment studies the case of the proton-odd nucleus  $^{51}\text{V}$ , using the  $(d, ^2\text{He})$  reaction to obtain  $\text{GT}^+$  strength distributions. The unbound diproton system is referred to as  $^2\text{He}$ , if the two protons couple to an  $^1S_0$ ,  $T = 1$  state. Experimentally, the  $^1S_0$  state is selected by limiting the relative energy of the two-proton system to 1 MeV, which is usually already guaranteed by the limited acceptance of the spectrometer. However,  $(d, ^2\text{He})$  reaction experiments are complicated due to the coincident detection of the two correlated protons in the presence of an overwhelming background originating from deuteron breakup. But as the reaction mechanism of  $(d, ^2\text{He})$  forces a spin-flip, the reaction is even more selective than  $(n, p)$  and  $(t, ^3\text{He})$  reactions, where non-spin-flip transitions can compete. A good basis for describing the interaction of a nuclear probe at intermediate energies is given by the effective nucleon-nucleon interaction of Love and Franey [14], which shows that in the kinematics region of low momentum transfer the  $\sigma\tau$  part of the interaction is by far the dominant term. This has recently been confirmed for the  $(d, ^2\text{He})$  reaction through experiments on  $p$ -shell and  $sd$ -shell nuclei [15–18].

The experiment was carried out using the ESN-BBS setup of the AGOR facility at KVI Groningen [19,20]. Deuterons of 171 MeV were delivered by the superconducting cyclotron AGOR. Beam line and Big-Bite magnetic spectrometer (BBS) were set up in dispersion-matched mode to ensure optimum energy resolution. The spectrometer was set to  $\Theta_{\text{BBS}} = 0^\circ$ . Beam currents were measured with a Faraday cup inside the spectrometer and ranged between 0.5 and 1.5 nA. Two self-supporting  $^{nat}\text{V}$  foils (99.75%  $^{51}\text{V}$ ) with thick-

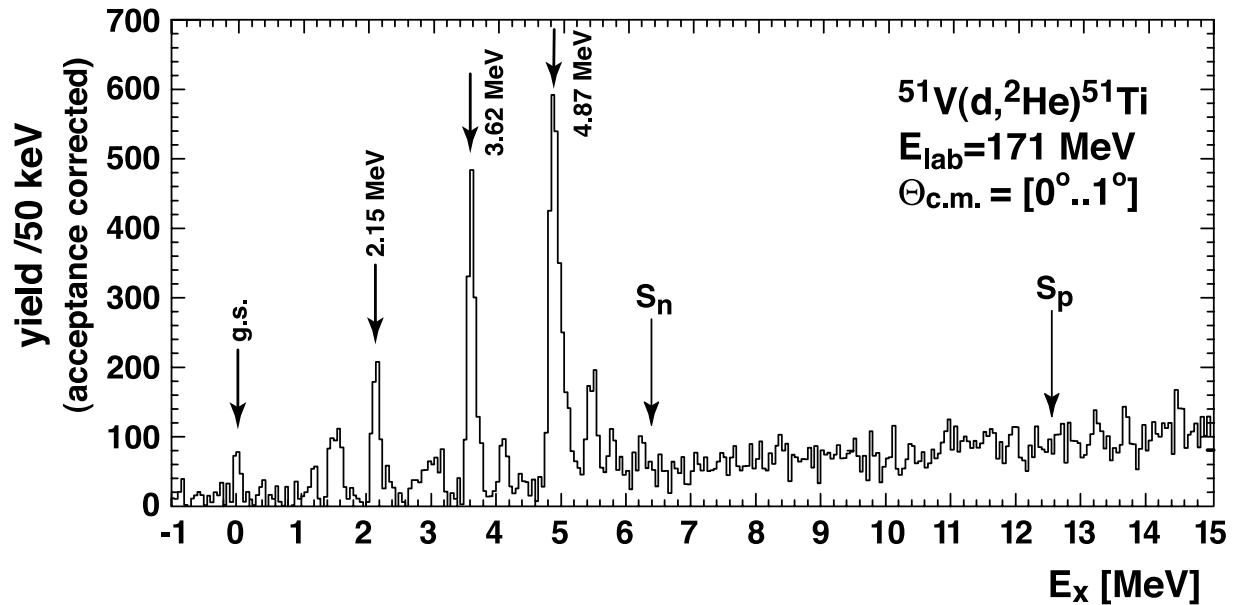


FIG. 1. Excitation energy spectrum for  $^{51}\text{V}(d,^2\text{He})^{51}\text{Ti}$ . The spectrum has been corrected for the acceptance of the spectrometer as detailed in Ref. [21]. The data were taken at a spectrometer setting of  $0^\circ$  covering a center of mass (c.m.) angular range between  $0^\circ$  and  $1^\circ$ . The energy resolution is 125 keV (FWHM).  $S_p$  and  $S_n$  denote the proton and neutron separation energies, respectively.

nesses of  $1.5 \text{ mg/cm}^2$  and  $4.3 \text{ mg/cm}^2$ , respectively, were used as targets. Reference measurements were taken with a  $^{12}\text{C}$  target (98.9%). The two outgoing protons were momentum analyzed by the BBS and detected in coincidence with the ESN detector. The ESN detector is a focal-plane detection system consisting of two vertical drift chambers and a set of four multiwire proportional chambers as an additional tracking detector. Reference [21] describes in detail how  $(d,^2\text{He})$  experiments with the BBS-ESN setup are being performed and analyzed.

The excitation energy spectrum, which was measured with the  $1.5 \text{ mg/cm}^2$  target covering scattering angles  $\Theta_{c.m.} \leq 2^\circ$ , was used to determine the peak positions with high precision. The fitting of the peaks was done manually supported by a  $\chi^2$  minimizing algorithm of the program FIT [22]. For this particular target an energy resolution  $\Delta E$  of 110 keV full width at half maximum (FWHM) was obtained for all peaks. Excitation energies up to the neutron separation energy of about 6.4 MeV were considered. The analysis was repeated with the excitation energy spectrum from the  $4.3 \text{ mg/cm}^2$  target. Because of the high statistics acquired with the thick target, the scattering angle could now be confined to  $\Theta_{c.m.} \leq 1^\circ$ . The corresponding excitation energy spectrum is shown in Fig. 1.  $\Delta E$  was about 125 keV (FWHM).

For the  $(n,p)$  and  $(p,n)$  elementary charge-exchange reactions at intermediate energies the measured cross section is connected to the GT strength [7,8]:

$$\frac{d\sigma(q=0)}{d\Omega} = \left( \frac{\mu}{\pi\hbar^2} \right)^2 \frac{k_f}{k_i} N_D J_{\sigma\tau}^2 B(\text{GT}). \quad (1)$$

Here,  $J_{\sigma\tau}$  denotes the volume integral of the spin-dependent isovector central part of the effective nucleon-nucleon inter-

action at  $q=0$  and can be obtained from Refs. [14,23]. The distortion factor  $N_D$  is usually determined by calculating the ratio between the distorted-wave and plane-wave cross sections. The proportionality of cross sections at  $q=0$  and  $B(\text{GT})$  for composite probes over a wide mass range is, e.g., shown in Ref. [9]. For the  $(d,^2\text{He})$  reaction an additional factor must be included, because here the cross section depends on the range of integration over the  $^2\text{He}$  internal energy [18], which is taken between 0 and 1 MeV.

The cross section  $d\sigma(q=0)/d\Omega$  is obtained by extrapolating the measured cross section to  $q=0$  using a DWBA (distorted-wave Born approximation) model calculation:

$$\frac{d\sigma(q=0)}{d\Omega} = \frac{\sigma_{calc}(q=0)}{\sigma_{calc}(\Theta, q)} \frac{d\sigma_{exp}(\Theta, q)}{d\Omega}. \quad (2)$$

The DWBA calculations for the present analysis were carried out with the code ACCBA [24]. The one-body transition densities were calculated in the formalism of normal modes assuming collective wave functions. These are regarded as superpositions of  $\nu$ -particle- $\pi$ -hole states. Optical model parameters from  $d+^{58}\text{Ni}$  at 170 MeV [25] were used for the entrance channel, and for the exit channel a global optical potential for  $p+^{51}\text{V}$  was extrapolated to 82 MeV [26]. The range of scattering angles and excitation energies considered here corresponds to momentum transfers  $q$  up to  $0.14 \text{ fm}^{-1}$ . For the extrapolation to  $q=0$  in Eq. (2), the calculations yield a factor that varies between 1.11 at  $E_x=0 \text{ MeV}$  and 1.49 at  $E_x=6.3 \text{ MeV}$ .

Although charge-exchange reactions near  $\Theta=0^\circ$  selectively proceed via GT transitions, there are usually small contributions from higher multipoles [see, e.g., the ground state (g.s.) transition in Fig. 1]. To identify transitions with  $\Delta L \geq 1$ , we employed the following procedure: The peak

TABLE I. Spectroscopic information and  $B(\text{GT})$  values. This table compares data from the present experiment (denoted as exp) with compiled data from Ref. [27] and the results from a shell-model calculation (SM). The experimental excitation energies were extracted from the spectrum presented in Fig. 1. The numbers within the brackets in this column denote the statistical errors in the last digits.  $B(\text{GT})$  values are given in units where  $B(\text{GT})=3$  for the decay of the neutron. The errors for  $B(\text{GT}^+)$  account for the statistical error and, in the case of individual transitions, for ambiguities in the fitting procedure. The systematic error, which is given by the uncertainties in the correction for the  $^2\text{He}$  detection probability, the extrapolation to  $q=0$ , and the error of  $S(\text{GT}^+)$  in Ref. [28], is evaluated to be 15%.  $\Delta L_{\text{min}}$  is the minimum transfer of angular momentum for the transition under consideration.

	$E_x$ (MeV)	$\Delta L_{\text{min}}$	$B(\text{GT}^+) \times 10^{-3}$	$E_x$ (MeV), $J^\pi$	$B(\text{GT}^+) \times 10^{-3}$	$\frac{B(\text{GT})_{\text{exp}}}{B(\text{GT})_{\text{SM}}}$
(exp)	(Ref. [27]), $J^\pi$		(exp)	(SM)	(SM)	
0.00(1)	0.00, $3/2^-$	2				
1.16(1)	1.17, $1/2^-$	2				
1.46(2)	1.44, $7/2^-$	0	} $60 \pm 6$	1.59, $7/2^-$	} 47	1.3
1.57(1)	1.57, $(5/2)^-$	0		1.55, $5/2^-$		
2.15(1)	2.14, $5/2^-$	0	$75 \pm 6$	2.08, $5/2^-$	110	0.7
2.33(1)	2.34, $11/2^-$	2				
2.72(3)	2.73, $(7/2, 9/2)^-$	0	} $57^a \pm 5$	2.82, $9/2^-$	} 47	1.2
2.90(3)	2.69, $7/2^-$	0		2.90, $5/2^-$		
	2.92, $(5/2, 7/2)^-$	0				
3.04(3)	2.92, $1/2^-$	2		3.36, $7/2^-$ ; 3.16, $9/2^-$		
3.04(3)	3.06, $(7/2, 9/2)^-$	0				
3.16(2)	3.17, $3/2^-$	2				
3.62(1)	3.62, $(5/2-9/2)^-$	0	$177 \pm 10$	3.71, $7/2^-$	211	0.8
3.77(1)	3.77, $9/2^+$	1				
4.09(1)	4.10, $(7/2, 9/2)$	0	} $74 \pm 6$	4.10, $9/2^-$	} 83	0.9
4.23(3)	4.19, $(5/2-9/2)$	0		3.89, $5/2^-$		
4.44(2)	4.46	(0)		4.44, $7/2^-$		
4.87(1)	4.89, $(5/2-9/2)^-$	0	$241 \pm 20$	4.81, $5/2^-$	400	0.6
4.99(3)	4.99; 5.00	(0)	$101 \pm 24$			
5.11(3)	5.14, $(5/2, 7/2)^-$	0	$49 \pm 15$	5.09, $7/2^-$	55	0.9
5.24(3)	5.21	(0)	} $288 \pm 12$	} $\left\{ \begin{array}{l} 5.22, 7/2^- \\ 5.53, 7/2^- \\ 5.59, 9/2^- \\ 5.68, 5/2^- \\ 5.68, 9/2^- \\ 5.77, 9/2^- \\ 6.33, 5/2^- \end{array} \right\}$	} $179 \pm 12$	} 1.6
5.42(2)	(0)					
5.54(2)	(0)					
5.78(3)	(0)					
5.95(3)	(0)					
6.14(3)	(0)					
6.25(3)	(0)					

<sup>a</sup>Possible contribution of  $\Delta L=2$ .

positions from our fit were compared with spectroscopic information from the literature [27]. Given the level density in  $^{51}\text{Ti}$  and the good energy resolution, the correspondence between the peak centroids with compiled data was unambiguous in most cases. The states that have  $J_f^\pi$  excluding a  $\Delta L=0$  transition were not considered in the final  $B(\text{GT}^+)$  distribution. The results are presented in Table I. The ground state of the initial ( $i$ ) nucleus  $^{51}\text{V}$  has  $J_i^\pi=7/2^-$ , thereby allowing GT transitions to  $J_f^\pi=5/2^-$ ,  $7/2^-$ , and  $9/2^-$ . Spectroscopic information is available for  $^{51}\text{Ti}$  up to  $E_x=5.22$  MeV, whereas discrete levels up to  $E_x \approx 6.3$  MeV are identified in the present analysis. Because of the restricted information on high-lying levels in  $^{51}\text{Ti}$ , the  $\Delta L=0$  charac-

ter of several weak transitions between  $E_x \approx 4.5$  MeV and  $E_x \approx 6.3$  MeV is assigned tentatively. For weak transitions which could not be resolved completely the summed strength of a group of neighboring levels is given. We estimate the uncertainty of the relative cross section in the interval  $0 \leq E_x \leq 6.3$  MeV to be about 10%. This uncertainty accounts for the Monte-Carlo simulation that corrects for the limited  $^2\text{He}$  detection probability of the experimental setup and the extrapolation to  $q \rightarrow 0$  with the DWBA calculation. We also considered the statistical error and, for individual peaks, an additional error due to ambiguities in the fitting procedure.

For the calibration of  $B(\text{GT}^+)$  we used the  $(n, p)$  reaction measurement on  $^{51}\text{V}$  at TRIUMF [28] as a reference. We

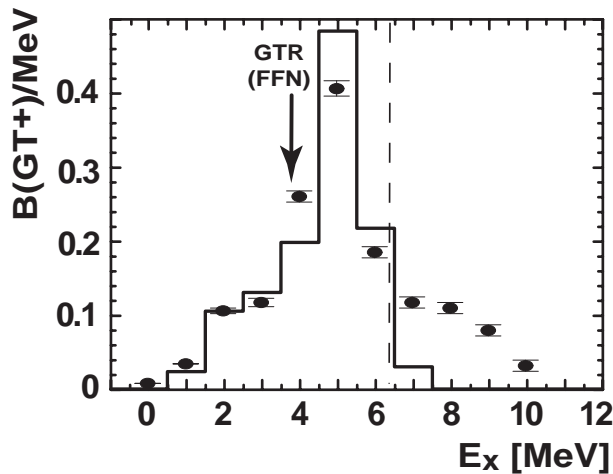


FIG. 2. Comparison between  $B(GT)$  distributions derived from the experimental cross sections measured in the  $(n,p)$  and  $(d,^2\text{He})$  reactions on  $^{51}\text{V}$ . The points indicate the result from the  $^{51}\text{V}(n,p)$  experiment at TRIUMF [28]. The histogram was obtained after folding the experimental  $B(GT)$  spectrum of Fig. 3 (top) with a Gaussian of 900 keV (FWHM) in order to compare with the TRIUMF data. The dashed line indicates the maximum excitation energy considered in the present analysis, as this defines the onset of a flat continuum response in the spectrum. The arrow denotes the position of the centroid of the GT resonance as predicted by FFN.

assume that the  $(n,p)$  experiment gives the summed strength  $S(GT^+)$  of the  $GT^+$  response whose fine structure is resolved through  $(d,^2\text{He})$ . A different prescription for calibrating the strength using the  $(d,^2\text{He})$  probe at 170 MeV has been given in Ref. [18] for the masses  $A=12$  and  $A=24$ . However, a simple extrapolation to  $A=51$  may not be reliable without having further data points in the medium-weight mass region and was therefore not attempted. The calibration was performed for  $0 \leq E_x \leq 5.0$  MeV, because in this excitation energy range the  $\Delta L=0$  transition strength can be extracted with high accuracy for both experiments considered here. Reference [28] reports  $S(GT^+) = 1.2 \pm 0.1$  for  $E_x \leq 8$  MeV. Limiting  $E_x$  to 5 MeV gives  $S(GT^+) = 0.9 \pm 0.1$ . The  $B(GT^+)$  spectrum derived from the  $^{51}\text{V}(n,p)$  experiment is shown in Fig. 2. The figure also contains the result of the present analysis, which was folded with the  $(n,p)$  experimental energy resolution to allow a direct comparison.

We note that  $GT^-$  strength from  $^{51}\text{V}$  has been measured in a  $(p,n)$  reaction study [29]. In a  $(p,p')$  experiment [30] a bump was observed at excitation energies where isospin-analog states to the  $GT^+$  transitions should appear ( $E_x \approx 10$  MeV). The spin-flip character was subsequently demonstrated by polarization measurements [31]. However, no individual transitions could be resolved in a high-resolution  $(e,e')$  experiment [32].

A shell-model calculation has been performed in the complete  $pf$  shell employing the KB3G interaction [33].  $B(GT^+)$  values were obtained adopting the Lanczos method with 100 iterations for each  $J_f^\pi$ . As  $0\hbar\omega$  shell-model calculations overestimate the experimental GT strength by a universal factor, we have scaled the GT strength by this factor  $(0.74)^2$  [34]. The result is shown in Fig. 3 (bottom). From these

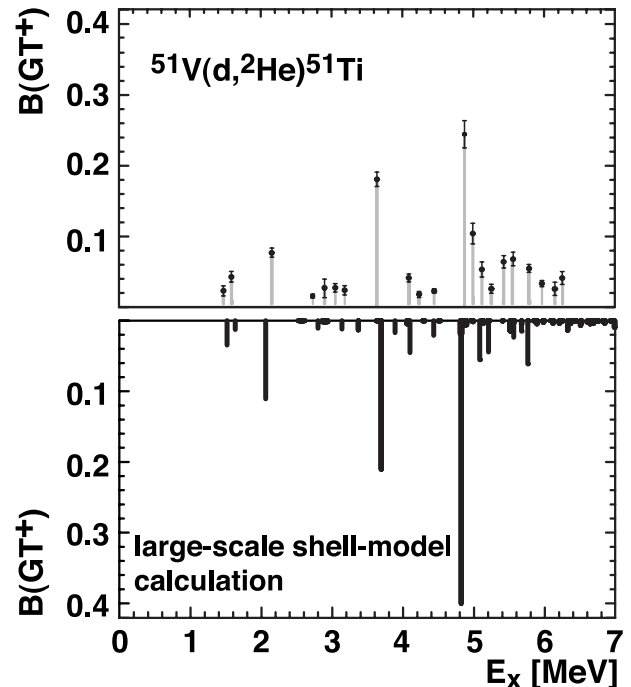


FIG. 3. Comparison between the  $(d,^2\text{He})$  reaction result (top) and the shell-model calculation (bottom). The error bars in the top figure indicate only the statistical errors. The relative strengths of transitions within the marked groups (see Table I) represent a possible interpretation of the spectrum in Fig. 1.

calculations one finds little strength above 6 MeV of excitation energy, which seems to be in accordance with our experimental observation. Table I presents the results of the calculations for the strongest transitions. Assignments of experimentally determined GT states to those theoretically calculated were done on the basis of proximity in excitation energy, spin, parity, and the size of the  $B(GT)$  values.

In Fig. 3 the experimental outcome is compared with the shell-model prediction, showing excellent agreement. It is interesting to compare the results with the early calculation of Fuller, Fowler, and Newman [3]. In the framework of the independent-particle model, a  $GT^+$  transition from  $^{51}\text{V}(\text{g.s.})$  corresponds to a transformation of the valence proton in the  $(1f_{7/2})$  subshell to a neutron in the  $(1f_{5/2})$  subshell. The simple single-particle model for  $^{51}\text{V}(\text{g.s.})$  is corroborated by the fact that its static magnetic moment ( $\mu = 5.15\mu_N$ ) [27] is close to the Schmidt value ( $\mu = 5.79\mu_N$ ). FFN assume that most of the strength is concentrated in a collective state, which is the GT resonance (GTR). The energy of the GTR above the ground state is given by the difference of the single-particle energies between the  $(2p_{3/2})$  and the  $(1f_{5/2})$  subshells. Furthermore, one has to take into account the particle-hole repulsion energy which must be paid when elevating the neutron from its ground state to the GT resonance state. These considerations yield  $E_x = 3.83$  MeV for the centroid of the GTR [35]. The centroid of the GT strength determined in the present experiment is at  $4.1 \pm 0.4$  MeV confirming the intuitive estimate of FFN (see Fig. 2).

To conclude, we have measured  $GT^+$  strength from the odd- $Z$  nucleus  $^{51}\text{V}$  up to  $E_x \approx 6$  MeV in the daughter nucleus

$^{51}\text{Ti}$  with an energy resolution of about 125 keV. The data have been compared with the prediction of a large-scale shell-model calculation. An interpretation in terms of the single-particle model is given.

In order to determine absolute  $\text{GT}^+$  strength independent of the outcome of the analog ( $n,p$ ) experiment, the calibration of ( $d,^2\text{He}$ ) reaction as a probe for  $B(\text{GT}^+)$  has to be extended to the medium-mass range. Furthermore, it still has to be clarified whether high-lying GT strength exists above 6 MeV of excitation energy. The identification will have to be

done on the basis of angular distributions and a multipole decomposition.

We wish to thank S. Brandenburg and the KVI accelerator staff. This work was performed with support from the Land Nordrhein-Westfalen and the EU under Contract No. TMR-LSF HPRI-1999-CT-00109. It was further performed as part of the research program of the Stichting FOM with financial support from the Nederlandse Organisatie voor Wetenschappelijk Onderzoek and as part of the research program of the Fund for Scientific Research-Flandres.

- 
- [1] F. Osterfeld, *Rev. Mod. Phys.* **64**, 491 (1992).  
 [2] H.A. Bethe, G.E. Brown, J. Applegate, and J.M. Lattimer, *Nucl. Phys.* **A324**, 487 (1979).  
 [3] G.M. Fuller, W.A. Fowler, and J. Newman, *Astrophys. J.* **293**, 1 (1985); *Astrophys. J., Suppl.* **48**, 279 (1982); *Astrophys. J.* **252**, 715 (1982); *Astrophys. J., Suppl.* **42**, 477 (1980).  
 [4] E. Caurier, K. Langanke, G. Martínez-Pinedo, and F. Nowacki, *Nucl. Phys.* **A653**, 439 (1999).  
 [5] K. Langanke, G. Martínez-Pinedo, and F. Nowacki, *Nucl. Phys.* **A673**, 481 (2000).  
 [6] K. Langanke and G. Martínez-Pinedo, *Rev. Mod. Phys.* **75**, 819 (2003).  
 [7] C.D. Goodman *et al.*, *Phys. Rev. Lett.* **44**, 1755 (1980).  
 [8] T.N. Taddeucci *et al.*, *Nucl. Phys.* **A469**, 125 (1987).  
 [9] M. Fujiwara *et al.*, *Nucl. Phys.* **A599**, 223c (1996).  
 [10] R. Helmer, *Can. J. Phys.* **65**, 588 (1987).  
 [11] K.P. Jackson *et al.*, *Phys. Lett. B* **201**, 25 (1988).  
 [12] B.M. Sherrill *et al.*, *Nucl. Instrum. Methods Phys. Res. A* **432**, 299 (1999).  
 [13] I. Daito *et al.*, *Phys. Lett. B* **418**, 27 (1998).  
 [14] M.A. Franey and W.G. Love, *Phys. Rev. C* **31**, 488 (1985).  
 [15] T. Niizeki *et al.*, *Nucl. Phys.* **A577**, 37c (1994).  
 [16] H. Ohnuma *et al.*, *Phys. Rev. C* **47**, 648 (1993).  
 [17] H.M. Xu *et al.*, *Phys. Rev. C* **52**, R1161 (1995).  
 [18] S. Rakers *et al.*, *Phys. Rev. C* **65**, 044323 (2002).  
 [19] A.M. van den Berg, *Nucl. Instrum. Methods Phys. Res. B* **99**, 637 (1995).  
 [20] H.J. Wörtche, *Nucl. Phys.* **A687**, 321c (2001).  
 [21] S. Rakers *et al.*, *Nucl. Instrum. Methods Phys. Res. A* **481**, 253 (2002).  
 [22] S. Strauch and F. Neumeyer, computer program FIT (TU Darmstadt, Germany, 1995).  
 [23] K. Nakayama and W.G. Love, *Phys. Rev. C* **38**, 51 (1988).  
 [24] H. Okamura, *Phys. Rev. C* **60**, 064602 (1999).  
 [25] C. Bäumer *et al.*, *Phys. Rev. C* **63**, 037601 (2001).  
 [26] A.J. Koning and J.P. Delaroche, *Nucl. Phys.* **A713**, 231 (2002).  
 [27] C. Zhou, *Nucl. Data Sheets* **81**, 183 (1997).  
 [28] W.P. Alford *et al.*, *Phys. Rev. C* **48**, 2818 (1993).  
 [29] J. Rapaport *et al.*, *Nucl. Phys.* **A427**, 332 (1984).  
 [30] C. Djalali *et al.*, *Nucl. Phys.* **A388**, 1 (1982).  
 [31] S.K. Nanda *et al.*, *Phys. Lett. B* **188**, 177 (1987).  
 [32] D. Bender *et al.*, *Nucl. Phys.* **A398**, 408 (1983).  
 [33] A. Poves, J. Sánchez-Solano, E. Caurier, and F. Nowacki, *Nucl. Phys.* **A694**, 157 (2001).  
 [34] G. Martínez-Pinedo, A. Poves, E. Caurier, and A.P. Zuker, *Phys. Rev. C* **53**, R2602 (1996).  
 [35] M.B. Aufderheide, S.D. Bloom, D.A. Resler, and G.J. Mathews, *Phys. Rev. C* **48**, 1677 (1993).